7.A6 POLYGONAL EYEWALLS IN A 2 KM WRF SIMULATION OF WILMA (2005)

Chris E. Blanton*
University of North Carolina at Charlotte
Charlotte, North Carolina

1. INTRODUCTION

The prediction of tropical cyclone (TC) intensity change remains a challenge. Track forecasting has improved steadily (Goerss 2006) largely due to improvements in global models, while full physics models with resolutions of a couple kilometers still often poorly predict intensity. The discrepancy exists because track prediction depends mostly on synoptic processes while intensity change depends on inner-core dynamics and the TC's relationship to its environment (Marks *et al*. 1998).

One inner-core process that models, in particular the Advanced Research Weather Research and Forecasting (WRF-ARW) model, may not resolve correctly is polygonal eyewalls. While TCs in nature have been observed taking a number of polygonal eyewall shapes (e.g. Lewis and Hawkins 1982), the polygonal eyewalls in WRF-ARW simulations are more numerous, higher-order, and often triangular (Corbosiero 2007; Davis *et al*. 2007). The reason that WRF-ARW seems predisposed to polygonal eyewalls is unknown, but the shapes probably affect the simulated TC's intensity due to the associated eye/eyewall mixing and asymmetrical convection.

This study examines the WRF output of a real-case simulation of Wilma that contains numerous polygonal eyewalls. Then a nondivergent barotropic model is initialized with snapshots of WRF symmetric vorticity to assess the relationship between the WRF shapes and the shapes that might arise purely due to barotropic influences.

2. WRF-ARW SIMULATION

The WRF-ARW model version 2.2 was used to simulate Wilma (2005). A telescoping 54/18/6/2 km domain set with two-way feedback was used; the 2 km domain covered an area of 592 km x 592 km, and the timesteps were 180/60/20/6.7 seconds. The vortex-tracking algorithm in WRF centered the 2 km domain every 15 minutes while the 6 and 18 km domains followed the 2 km domain. The 1º initial conditions for the 1800 UTC 17 October 2005 GFS run were used to initialize the WRF model; no bogus vortex was used as the initial vortex was weak and approximately accurate. Physical parameterizations included the WRF Single-Moment 6-class microphysics, the Kain-Fritsch cumulus (only for the 54 and 18 km domains), and the Yonsei University planetary boundary layer.

The simulated Wilma intensified for 72 hours (Fig. 1), and the intensification rate of 2 hPa h^{-1} between 0600-1800 UTC 19 October compares well with other WRF and MM5 real-case simulations (e.g.

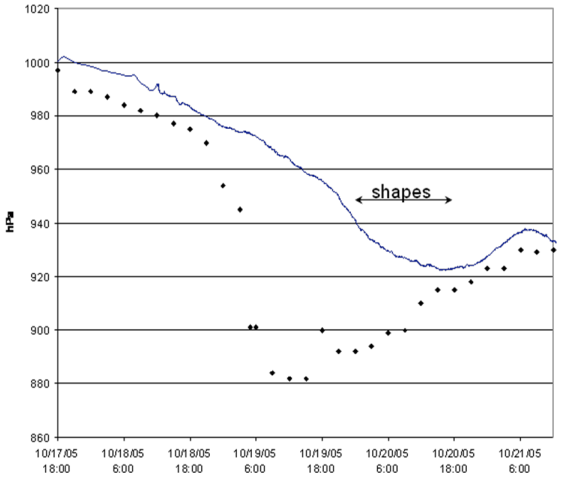

Fig. 1. Minimum surface pressure (hPa) for the real (diamonds) and WRF (line) Wilmas. The simulated Wilma shows strong eyewall shapes between 0000-1800 UTC 19 October.

Davis *et al*. 2007). Although some WN 3-5 growth was evident during this period of intensification (Fig. 2), much stronger and somewhat unrealistic shapes appeared as the intensification slowed (e.g. Fig. 3a); the shapes included triangles, squares, and pentagons, and persisted for 18 hours. Corbosiero (2007) suggested that the unusual eyewall shapes result in anomalously weak TCs; the temporal connection between the strong eyewall shapes and a slowing of intensification here would seem to support that suspicion.

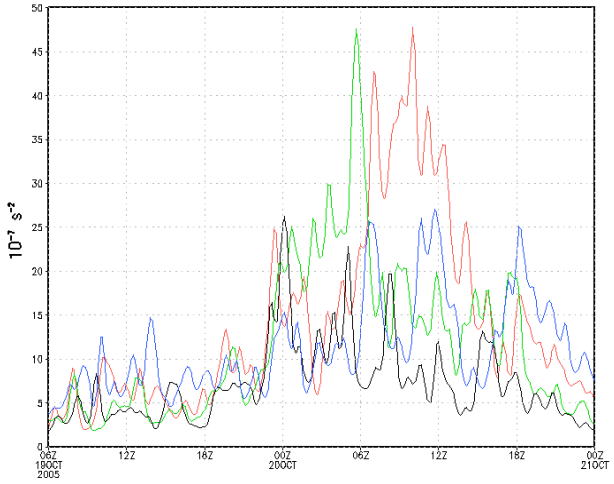

Fig. 2. Azimuthal power spectra (10^{-7} s^{-2}) for WN 2 (blue), 3 (red), 4 (green), and 5 (black) averaged between r = 24-36 km at 750 m.

* *Corresponding author address:* Chris E. Blanton, University of North Carolina, Department of Geography and Earth Sciences, Charlotte, NC 28223; email: ceblanton@gmail.com

3. NONDIVERGENT BAROTROPIC SIMULATIONS

The favored azimuthal wavenumber growth tendencies of the simulated Wilma's background flow were diagnosed at a number of times using a nondivergent barotropic model. The nondivergent barotropic model was first used to investigate polygonal eyewalls by Schubert *et al*. (1999), and the barotropic model used here is nearly identical to theirs. The double Fourier pseudospectral model uses a Cartesian grid of 512 x 512 collocated points covering 600 km x 600 km, 170 Fourier modes, a timestep of 7.5 seconds, and a diffusion coefficient of 10 m^2 s^{-1}. Although the grid points are 1.17 km apart, the effective resolution is limited by the highest Fourier mode, 3.53 km.

The WRF model times used to initialize the barotropic model were somewhat arbitrarily chosen to be every hour between 0600 UTC 19 October and 0000 UTC 21 October—42 times. Two vertical levels were used, the 310 and 318 K isentropic levels, which were ~1 and 2 km in height. The inner 150 km of the symmetric vorticity profile was used to initialize the barotropic model; the rest of the domain was set to be slightly negative so that the vorticity sum of the domain was zero. Random noise of amplitude ~10^{-5} s^{-1}, or ~1% of the annular ring vorticity, was added to the area within 100 km of the TC center. However, in some cases reducing the amplitude of the noise resulted in substantially different simulations, so the details of the initial noise may need to be revisited. The barotropic simulations were run for 24 hours, long enough for most of the rings to break into mesovortices.

At the 310 K level, the level of maximum vorticity perturbation amplitudes, the dominant wavenumber growths in the barotropic simulations showed moderate agreement with the WRF shapes at the times of the initial conditions. Based on the highest Fourier power spectra in the WRF simulation and the observed growth in the barotropic simulation, out of the 42 times, the WRF (barotropic) simulation showed WN 2 11 (10) times, WN 3 17 (9) times, WN 4 7 (11) times, WN 5 7 (7) times, WN 6 0 (3) times, WN 7 0 (1) time(s), and WN 8 0 (1) time(s). Although overall the barotropic simulations were biased towards higher wavenumbers, the barotropic growth matched the dominant WRF wavenumber 14 times and was off by one wavenumber another 14 times.

Many of the barotropic simulations contained a WN 1 “pulse” that rotated on top of the dominant wavenumber development and caused a variety of chaotic mischief. Before wave-breaking the pulse disrupted and slowed the unstable growth; during wave-breaking it sometimes caused the instability to break as one wavenumber smaller. After the mesovortices broke, the pulse became a wobble that encouraged mesovortex merger and made the mesovortex configuration more asymmetrical. One asymmetrical configuration was a trapezoid, interesting as the WRF simulation also contained a trapezoid (Fig. 3). Because Schubert *et al*'s (1999) simulation did not contain a pulse and the barotropic model correctly reproduced the simulation of Schubert *et al*. (1999) using their initial conditions,

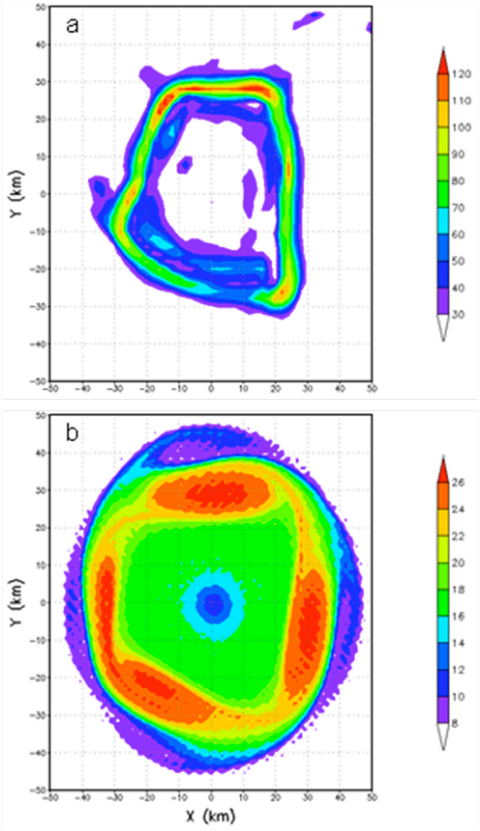

Fig. 3. Vorticity (10^{-4} s^{-1}) from the (a) WRF model (0902 UTC 20 October, 750 m) and (b) barotropic model (simulation hour 22:00, initialized from 310 K WRF output at 0900 UTC 19 October).

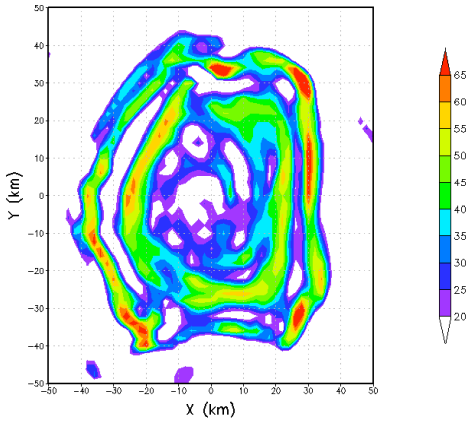

Fig. 4. WRF 318 K vorticity (10^{-4} s^{-1}) at 1600 UTC 20 October.

the pulse likely results from the model initialization, either the symmetric vorticity profile or the random noise. The WN 1 “inner-core” instability of Nolan and Montgomery (2000) could also be involved.

The symmetric vorticity at the 318 K level often contained two rings (e.g. Fig. 4); the inner ring appeared to result from repeated partial collapses of the primary (outer) ring. Consequently, 18 of the 318 K barotropic simulations showed double-ring instabilities (Kossin *et al*. 2000). Most (12) of these

simulations were initialized with an inner ring stronger than the outer ring, and resulted in a WN 2 Type 2 instability similar to Kossin *et al*.'s (2000) Fig. 13. In four others the rings were of equal amplitude, and resulted in high wavenumber (5-10) Type 2 instabilities.

Two simulations were initialized with an outer ring stronger than the inner ring, and these had characteristics of both Type 1 and Type 2 instabilities. Early in these simulations, perturbations along the inner and outer edge of the outer ring phase-locked and grew, affected remotely by the inner ring (Type 1 instability). Later, mesovortex development in the inner ring directly affected the outer ring mesovortices across the moat (Type 2 instability). In one case, the phase speeds of the inner (WN 5) and outer (WN 10) ring mesovortices were equal so that the Type 2 instability affected only half of the outer ring mesovortices, causing them to grow quicker (Fig. 5). In the other case, the two sets of mesovortices rotated at different phase speeds, resulting in equal Type 2 instability influence on the outer ring mesovortices.

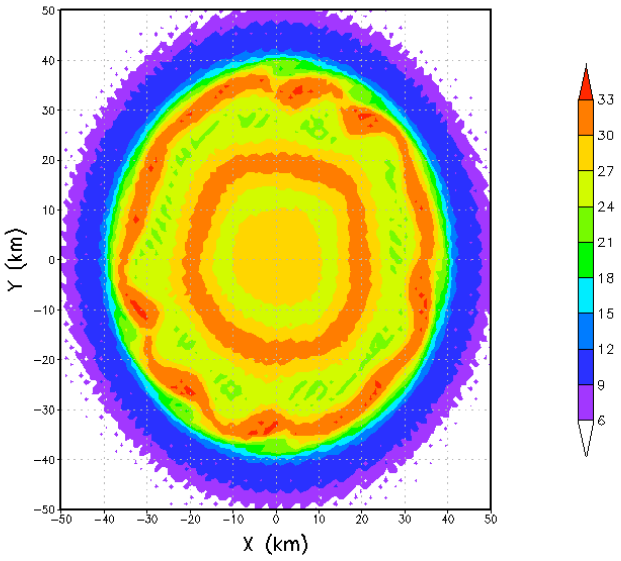

Fig. 5. Vorticity (10^{-4} s^{-1}) at simulation hour 18:50 from barotropic model initialized from 318 K WRF output at 0100 UTC 20 October.

4. **REFERENCES**

Corbosiero, K. L., 2007: Advanced Research WRF high resolution simulations of the inner core structures of Hurricanes Katrina, Rita, and Wilma (2005). Proceedings, *8th Annual WRF Users Workshop*, Boulder, CO, NCAR.

Davis, C, W. Wang, S. Chen, Y. Chen, K. Corbosiero, M. DeMaria, J. Dudhia, G. Holland, J. Klemp, J. Michalakes, H. Reeves, R. Rotunno, and Q. Xiao, 2007: Prediction of landfalling hurricanes with the Advanced Hurricane WRF model. *Mon. Wea. Rev*., Accepted.

Goerss, J. S., 2006: Prediction of tropical cyclone track forecast error for Hurricanes Katrina, Rita, and Wilma. Preprints, *27th AMS Conference on Hurricanes and Tropical Meteorology*, Monterey, CA, Amer. Meteor. Soc., 11A.1.

Kossin, J. P., and W. H. Schubert, and M. T. Montgomery, 2000: Unstable interactions between a hurricane's primary eyewall and a secondary ring of enhanced vorticity. *J. Atmos. Sci.*, **57**, 3893-3917.

Lewis, B. M., and H. F. Hawkins, 1982: Polygonal eye walls and rainbands in hurricanes. *Bull. Amer. Meteor. Soc*., **63**, 1294-1301.

Marks, F. D. and L. K. Shay, 1998: Landfalling tropical cyclones: Forecast problems and associated research opportunities. *Bull. Amer. Meteor. Soc.*, **79**, 305–323.

Nolan, D. S., and M. T. Montgomery, 2000: The algebraic growth of wavenumber one disturbances in hurricane-like vortices. *J. Atmos. Sci.*, **57**, 3514-3538.

Schubert, W. H., M. T. Montgomery, R. K. Taft, T. A. Guinn, S. R. Fulton, J. P. Kossin, and J. P. Edwards, 1999: Polygonal eyewalls, asymmetric eye contraction, and potential vorticity mixing in hurricanes. *J. Atmos. Sci.*, **56**, 1197-1223.